# Externally Phase Locked Submm-Wave Flux Flow Oscillator for Integrated Receiver

**V.P. Koshelets[1], A.B. Ermakov[1], S.V. Shitov[1], P.N. Dmitriev[1], L.V. Filippenko[1], A.M. Baryshev[2], W. Luinge[2], J. Mygind[3], V.L. Vaks[4], D.G. Pavel'ev[5]**

[1] Institute of Radio Engineering and Electronics (IREE), Russian Academy of Sciences, Mokhovaya 11, GSP-3, 103907 Moscow, Russia (e-mail: valery@hitech.cplire.ru)

[2] Space Research Organization of the Netherlands (SRON)
P.O. Box 800, 9700 AV Groningen, the Netherlands

[3] Department of Physics, Technical University of Denmark,
B 309, DK-2800 Lyngby, Denmark

[4] Institute for Physics of Microstructure, Russian Academy of Sciences,
GSP-105, 603600 Nizhny Novgorod, Russia

[5] Nizhny Novgorod State University,
Gagarin Avenue 23, 603600 Nizhny Novgorod, Russia

## ABSTRACT

The combination of narrow linewidth and wide-band tunability makes the Josephson Flux Flow Oscillator (FFO) a perfect on-chip local oscillator for integrated submm-wave receivers. A noise temperature of about 100 K (DSB) has been achieved for the integrated receiver with the FFO operating near 500 GHz. An instantaneous bandwidth of 15 – 20 % is estimated from Fourier transform spectroscopy (FTS) and heterodyne measurements. The far-field antenna beam is measured as $\approx$ f/10 with sidelobes below -16 dB which is suitable for coupling to a telescope antenna. For application in spectral radio astronomy, besides low noise temperature and good beam pattern, also a local oscillator with narrow-linewidth and long-term stability is required. Recently the feasibility of phase locking of the FFO to an external reference oscillator was demonstrated experimentally. A spectral linewidth as low as 1 Hz (determined by the resolution of the spectrum analyzer) has been measured in the frequency range 270 - 440 GHz relative to a reference oscillator. This linewidth is far below the fundamental level given by shot and thermal noise of the free-running tunnel junction. A new technique for linewidth measurements and FFO phase locking has been devised and put to use. This method employs an off-chip harmonic multiplier that considerably simplifies the design of the chip for a fully superconductive integrated phase-locked receiver. The linewidth of Nb-AlO$_x$-Nb FFOs has been carefully studied in the frequency range 250 - 600 GHz. Based on frequency measurements the FFO I-V curve has been reconstructed with an accuracy better than 1 nV. Finally, the results of FFO phase noise measurements are also presented and discussed.

## 1. Introduction

Light-weight and compact ultrasensitive submm-wave Superconducting Integrated Receivers (SIRs) with low power consumption [1,2] are very attractive for both radio-astronomical research and remote monitoring of the Earth atmosphere. The new ambitious radio-astronomy multi-dish projects (e.g., ALMA) would gain considerably by using single-chip SIRs due to their lower price and better serviceability as compared to conventional approaches. Present single-chip superconducting receivers comprise a SIS-mixer with a quasioptical antenna and a superconducting local oscillator (LO).

Presently, a Flux Flow Oscillator (FFO) based on unidirectional flow of magnetic vortices in a long Josephson tunnel junction [3] looks most promising as LO for on-chip integration with a SIS mixer. Nb-AlO$_x$-Nb FFOs which have been successfully tested from about 120 to 700 GHz - gap frequency of Nb - deliver sufficient power ($\approx$1 $\mu$W at 450 GHz) to pump a SIS mixer. Both frequency and power of the FFO can be tuned electronically [4,5]. A receiver noise temperature below 100 K (DSB) has been achieved for a SIR with an internal FFO operated in the frequency range 480 - 520 GHz [1,2]. This means that the performance of the SIS mixer is close to the quantum limit. A FFO can be fabricated on the same trilayer - and by the same technological procedure - as a SIS mixer. Further, the complexity of a FFO circuit is much lower than known Josephson junction array oscillators. A free-running FFO linewidth considerably below 1 MHz has been measured near 450 GHz [6-8]. Recently the feasibility of phase locking of the FFO to an external oscillator was demonstrated experimentally [7,8].

In this report we present an overview of the basic FFO properties as well as the latest FFO linewidth measurements - including FFO phase noise. We also describe a new technique for linewidth measurements and FFO phase locking.

## 2. Flux Flow Oscillators: dc properties and linewidth measurements.

The FFO [3] is a *long* overlap Josephson tunnel junction in which an applied dc magnetic field and a uniformly distributed dc bias current, $I_b$, drive a unidirectional flow of fluxons, each containing one magnetic flux quantum, $\boldsymbol{F_0} = h/2e \approx 2\ 10^{-15}$ Wb. Symbol $h$ is Planck's constant and $e$ is the electron charge. A dc current, $I_{CL}$, in an external coil or an integrated control line generates the magnetic field, $B_{appl}$, applied perpendicular to the FFO. According to the Josephson relation a FFO biased at voltage $V$ oscillates with frequency $f = (2\boldsymbol{p}/\boldsymbol{F_0})\ V$ (about 483.6 GHz/mV). Velocity and density of the fluxons, and thus the power and frequency of the emitted mm-wave signal can be adjusted by $I_b$ and $I_{CL}$.

The FFOs considered below are long Nb-AlO$_x$-Nb tunnel junctions with overlap geometry (see inset in Fig. 1). The length, $L$, and the width, $W$, are about 500 $\mu$m and 3 $\mu$m, respectively. The critical current density, $j_c$, is in the range 4 - 8 kA/cm$^2$, which corresponds to a specific resistance, $R_n*L*W \approx 50 - 25\ \Omega\ \mu$m$^2$ (the Josephson penetration depth $\boldsymbol{l}_J \approx 6 - 4\ \mu$m). The tunnel barrier usually is formed in a long window of a relatively thick insulation layer (200 - 350 nm, SiO$_2$) between two superconducting Nb films (base and counter electrodes). One of the electrodes also is employed as control line.

A typical set of current-voltage characteristics (IVCs) of the FFO, measured at different magnetic fields ($I_{CL}$), is shown in Fig. 1. Simultaneously with recording the IVCs, the power delivered by the FFO to the integrated SIS detector was measured by a data acquisition system, IRTECON [1, 2]. The criterion for sufficient pumping is a pre-set change of the subgap tunnel current at $V = 2$ mV, $DI$, relative to the gap current $I_g$ of the SIS detector, due to photon assistant tunneling (PAT). A $DI/I_g$-ratio exceeding 0.25 was obtained for FFO voltages from 550 to 1070 $\mu$V (see arrow in Fig. 1). This corresponds to a frequency range 270 - 520 GHz. Actually, the operational frequency range is limited by the matching circuit and the SIS tuning structure rather than by the FFO itself.

A detailed study of long Josephson junctions intended for wide-band integrated oscillators was performed [9]. At large fields and voltages (Fig. 1) one can see the smooth so-called Flux Flow Step (FFS), the voltage of which is proportional to $I_{CL}$. At moderate fields the FFS splits into a series of resonant Fiske steps (FS) [10]. This resonant mode exists up to a specific "boundary" voltage, $V_{JSC}$, at which a "bump" in dc current appears. As also seen from Fig. 1 for $V > V_{JSC}$ the FFS becomes smooth and with increasing magnetic field it persists up to the gap voltage. It should be noted that this "boundary" is typical for all investigated FFOs with high current density ($j_c > 1$ kA/cm$^2$). This feature neither depends significantly on the junction geometry and its dimensions nor on the coupling to the external microwave circuit.

The boundary voltage is about 930 $\mu$V which is 1/3 of the superconductor gap voltage $V_g$ for Nb-AlO$_x$-Nb tunnel junctions. This threshold behavior has been explained
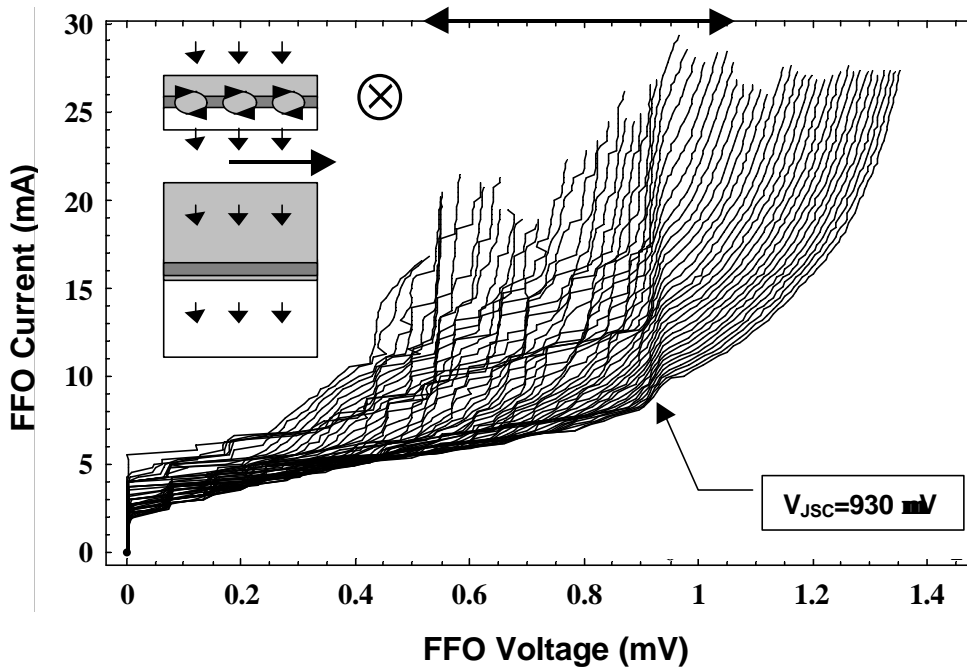


**Fig. 1.** IVCs of a Nb-AlO$_x$-Nb FFO recorded at different magnetic fields. Note the abrupt change of the IVC at the boundary voltage $V_{JSC} \approx 930$ $\mu$V. Insets show the cross section of the long junction with driven vortices (top) and its overlap geometry (bottom).

by Josephson self-coupling (JSC) [9]. The JCS effect is basically absorption of *ac* radiation by the quasi-particles in the cavity of the long junction. The JSC results in current bumps (similar to PAT quasi-particle steps in a SIS mixer) at $V_{JSC} = V_g/(2n + 1)$, which gives $V_{JSC} = V_g/3$ *for n = 1*. The effect of self-pumping explains not only the bumps observed in the FFO IVC, but also the abrupt merge of Fiske steps (suppression of the resonant Fiske mode for $V \, ^3 V_g/3$) caused by a strong increase of the internal damping due to quasi-particle tunneling [9].

A specially designed integrated circuit is used for linewidth measurements [7, 8]. It comprises FFO, SIS mixer and elements for rf coupling - see Fig. 2. The signal from the FFO is applied to the harmonic mixer (a SIS junction operated in Josephson or quasiparticle mode) along with the signal from a frequency synthesizer, $f_{SYN} \approx 10$ GHz. In order to prevent the synthesizer signal (as well as its lower harmonics) from reaching the FFO a high-pass microstrip filter with cut-off frequency about 200 GHz is inserted between the FFO and the harmonic mixer. The intermediate frequency (IF) signal with frequency, $f_{IF} = \pm (f_{FFO} - n \, f_{SYN})$ is boosted first by a cooled amplifier and then by a room-temperature amplifier for further use in the PLL system. A part of the signal is applied via a directional coupler to a spectrum analyzer which is also phase locked to the synthesizer using a common reference signal at 10 MHz. Thus, the spectrum observed in the IF channel, as well as the phase noise evaluated from these data, is the difference between the frequency of the FFO signal and the n-th harmonic of the synthesizer frequency.

The output signal of the PLL system - proportional to the phase difference - is returned via the Loop Bandwidth Regulator (maximum bandwidth about 10 MHz) to the FFO via a coaxial cable terminated with a cold $50 \, \Omega$ resistor mounted on the chip bias plate. It was proven experimentally that the PLL system can considerably narrow the FFO linewidth if $Df_{AUT}$ (measured at the -3 dB level) is smaller than the PLL regulation bandwidth, $B_{PLL}$. Figure 3 [7] shows typical IF power spectra of the phase locked FFO
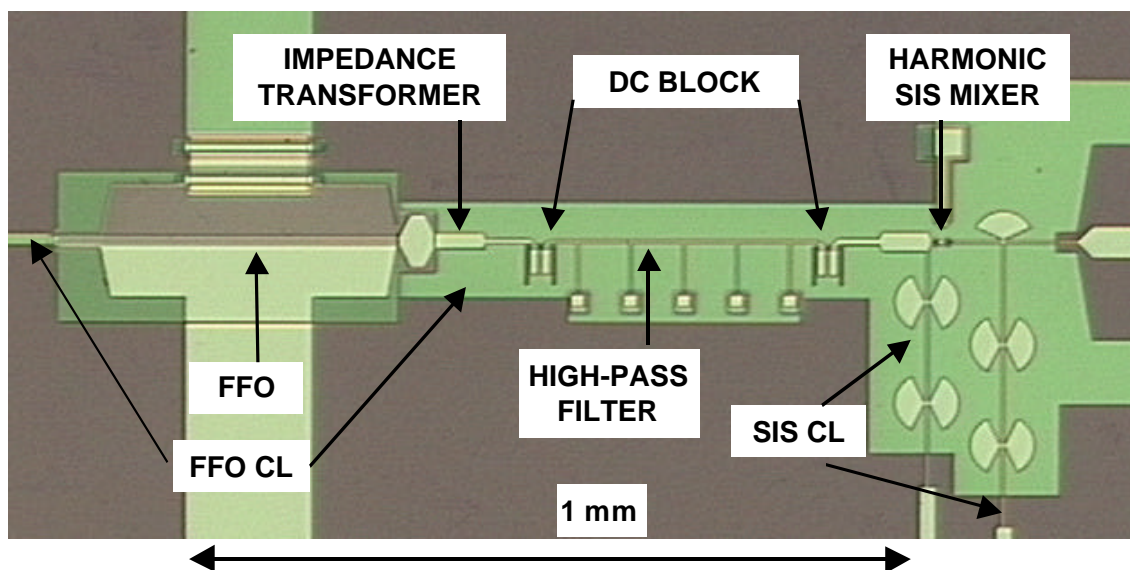


**Fig. 2.** Central part of the microcircuits used for FFO linewidth measurements.

measured at $f_{FFO}$ = 439 GHz for different settings of the spectrum analyzer. A FFO linewidth as low as 1 Hz is presented in Fig. 3b; it is limited by the resolution bandwidth of the spectrum analyzer. This experimental results show that the FFO linewidth can be reduced below the value determined by the fundamental shot and thermal fluctuations of the free-running tunnel junction. To our knowledge it is the first time such a dramatic reduction of the initial linewidth of a Josephson oscillator has been achieved.
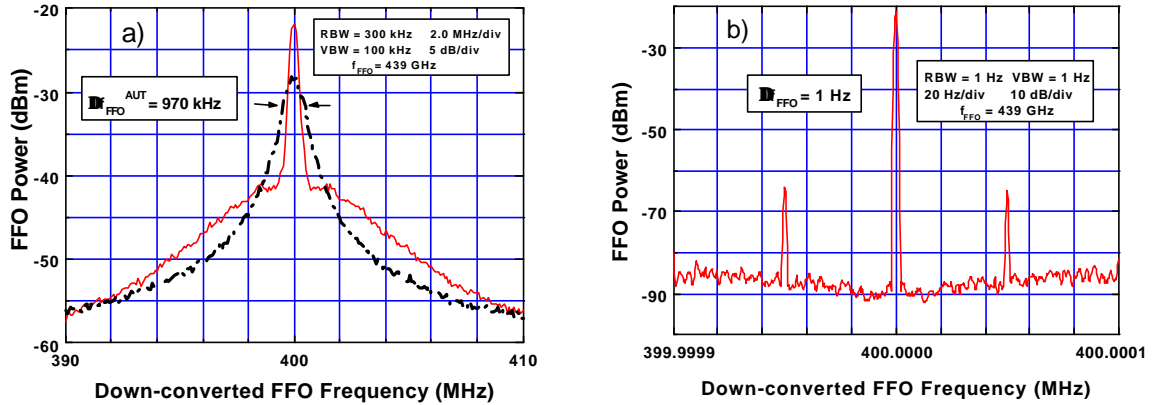


**Fig. 3.** [7] The down-converted IF power spectra of the FFO (f = 439 GHz), recorded with different frequency spans, clearly demonstrate the phase locking.

The residual phase noise of the phase locked FFO - measured relative to the reference synthesizer - is plotted in Fig. 4 for three different FFO frequencies as function of the offset from the 400 MHz carrier. One can see that there is no pronounced dependence of the phase noise on the frequency of the locked FFO. It means that the noise is mainly controlled by the measuring technique and the PLL system. To get the total FFO phase noise, one should add the synthesizer noise multiplied by $n^2$ to residual phase noise of the FFO. The measured data for the used synthesizer (HP83752B) are also presented in Fig. 4. In this measurement where the FFO, operating at 387 GHz, is locked to the 36-th harmonic of the synthesizer, $n^2$ = 1296. The total FFO phase noise (solid line in Fig. 4) is dominated by the synthesizer noise for offsets < 100 kHz. The origin of the noise at larger frequency offset is under investigation.

It should be noted that phase locking of a FFO has been realized only on the steep FSs, where the free-running FFO linewidth is about 1 MHz corresponding to small values of $R_d^B$ and especially $R_d^{CL}$, where $R_d^B = \partial V_{FFO}/\partial I_b$ and $R_d^{CL} = \partial V_{FFO}/\partial I_{CL}$ are the differential resistances associated with the bias current, $I_b$, and the control-line current, $I_{CL}$, respectively. The linewidth increases at voltages above the boundary voltage, $V_{JSC}$, [9] where $R_d^B$ and $R_d^{CL}$ are considerably larger than on the Fiske steps (as a result of the abrupt increase of internal damping due to Josephson self-coupling [9]). It is still an experimental challenge to obtain phase locked operation in the "true" flux flow regime where the normalized damping is large, $\alpha L/l_J \geq \pi$, and correspondingly, the initial FFO linewidth exceeds $\approx$10 MHz.
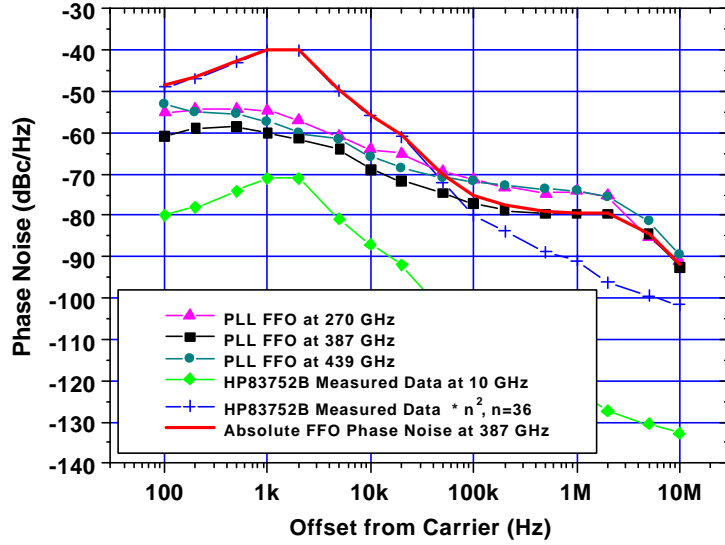
**Fig. 4.** Experimental phase noise of a phase locked FFO at different frequencies. Since the phase noise of the FFO, e.g., at 387 GHz is measured relative to the 36th harmonic of the synthesizer, the synthesizer noise, multiplied by a factor $36^2 = 1296$, should be added to residual FFO noise to get the total (absolute) FFO phase noise – solid line.

## 3. Super-fine Structure of the FFO IVCs; External Harmonic Multiplier.

Previous FFO linewidth measurements [6,11] have demonstrated the existence of a structure of closely spaced steps in the IVC of long Josephson junctions. The voltage spacing is about 20 nV, corresponding to a frequency separation of 10 MHz, that cannot be recorded by usual dc technique. This structure manifests itself as a nonlinear relation between the measured FFO frequency and the bias or/and control-line currents. Actually, an FFO can irradiate only in a specific range near the corresponding "resonance" frequencies, $f_r$, while the oscillator is unstable between these values. This behavior is clearly demonstrated in Fig. 5 ($f_{synt} = 17.05$ GHz, $n = 25$, Lower Side Band). Traces A and B are recorded at constant bias current: $I_b = 17\,782$ µA and $17\,779$ µA, respectively (number of averages, $N_{av} = 100$). Point A is stable while an attempt to bias at point B fails due to small fluctuations which force the FFO to jump between stable states, spending on the average almost equal time in both states (see curve B).

Figure 6 illustrates this phenomenon in a different way. Trace A is – as above – the down-converted signal of the FFO biased at a stable point, while trace B is recorded when fine-tuning the FFO bias (from 18 710 µA to 18 770 µA) in the regime "max-hold". In this regime the spectrum analyzer takes the maximum signal amplitude from many measurements at each frequency point. One can see that FFO frequency can be permanently tuned only in a range of about 5 MHz, while frequencies between these stable regions cannot be obtained. Even a small change of the bias current near the edge of the stable region, the frequency (voltage) of the FFO "jumps" to the next stable region. Note that a 50 MHz frequency shift (which is equivalent to a voltage difference of 100 nV) was obtained for a current change of 60 µA, that corresponds to "averaged" $R_d^B = 0.0017$ Ω.
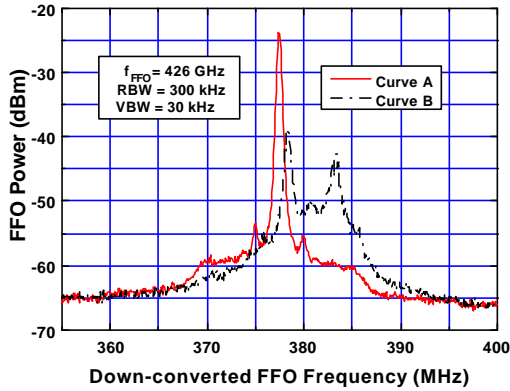
**Fig. 5**. Down-converted FFO signal recorded at constant bias current adjusted inside one of the resonances (curve A) and in between two resonances (curve B).
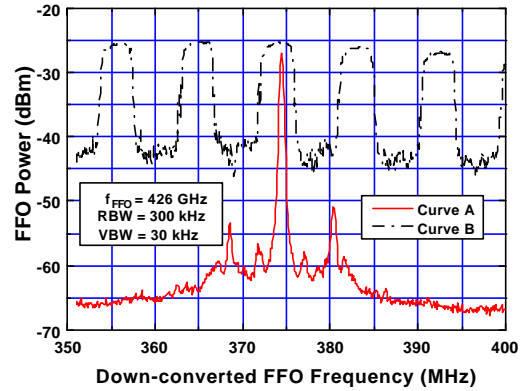
**Fig. 6**. Down-converted FFO signal recorded at fixed bias current inside one of the resonances (curve A) and with the FFO bias tuned in the "max hold" regime (curve B).

Using the Josephson equation the FFO IVC can be reconstructed in detail by measuring the bias current dependence of the FFO output frequency. The accuracy of the frequency (and correspondingly, voltage) measurement can be very high if, e.g., a synthesizer is used as a reference source. Actually, the accuracy is determined by the spectrum analyzer resolution used for the specific span. For the data presented in Fig. 5-8 the resolution bandwidth, RBW, was 300 kHz corresponding to a voltage accuracy of about 0.6 nV. By using a special measuring procedure the frequency reading from the spectrum analyzer was recorded simultaneously with adjusting $I_b$ and $I_{CL}$. The measured dependence of the down-converted FFO frequency on $I_b$ is shown in Fig. 7. The data sets marked #01, #02 and #03 are recorded at slightly different values of $I_{CL}$ (what results in jumping to the adjacent resonances and small shift along the $I_b$-axis). From these data the exact shape of the FFO can be reconstructed; the "recovered" FFO IVCs demonstrate the existence of well-defined superfine structure (see Fig. 8). Up to now there is no reliable theoretical explanation of this superfine resonant structure. The exact geometry of the FFO influences the resonant structure, in particular, the results presented in Fig. 3 [7, 8] were measured for a tapered FFO where the resonance effect was less pronounced. The results depicted in Figs. 5-8 are from an FFO with a standard rectangular geometry.

From Fig. 8 one can see that the FFO IVC (at low levels of external interference) consists of a set of separate steps rather than being a continuous curve. The differential resistance on these steps is extremely low, $R_d^B(res) = 0.00037\ \Omega$. Important to note is, that this value is considerably lower than the average value ($R_d^B = 0.0016\ \Omega$) recorded using the traditional technique. An even more dramatic reduction has been measured for the control-line differential resistance, $R_d^{CL} = \P V_{FFO}/\P I_{CL}$.

Since the frequency separation between adjacent resonances is comparable with the maximum PLL system bandwidth, jumps between adjacent resonances create considerable difficulties for phase locking of the FFO. Nevertheless full phase locking can be realized even in the presence of the resonance structures but only at specific frequencies (see Fig. 9, 10).
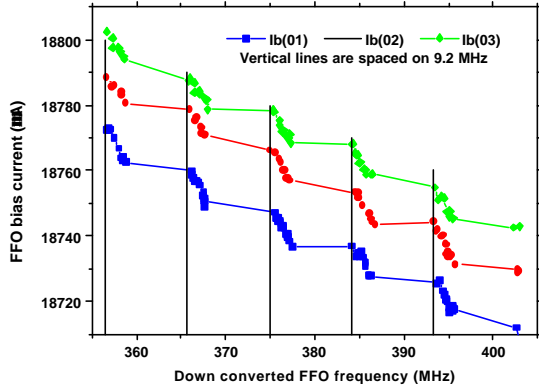
**Fig. 7.** Down-converted FFO frequency versus FFO bias current at slightly different control line currents. Note that the absolute positions of the resonances (and the distance between adjacent resonances) are the same for all curves.
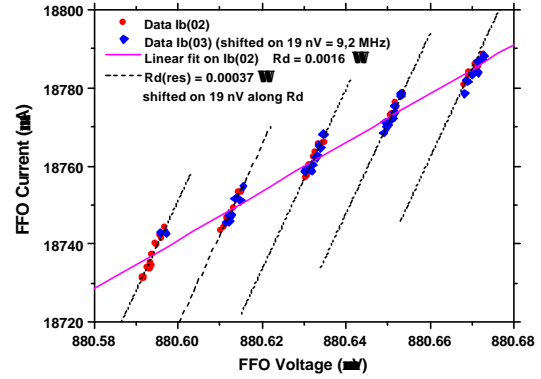
**Fig. 8**. Reconstructed IVC of the FFO. Data #03 are measured at a slightly different $I_{CL}$ and corresponds to an adjacent resonance. These data are shifted by 19 nV along the Fiske step with slope $1/R_d^B$.

In order to exclude that the recorded resonance structure could be due to the integrated harmonic mixer technique, an external harmonic multiplier based on a quasi-planar superlattice electronic device (SLED) [12] has been developed and tested. The SLED was mounted in a circular waveguide (with a cut-off frequency of about 400 GHz) followed by a conical horn with an output diameter of 6 mm. A constant-voltage bias and the pump signal from the synthesizer (frequency 1 - 30 GHz) are applied to the SLED. The signal of multiplier is fed to an integrated receiver of standard design [1,2] via a vacuum window. Heterodyne mixing with the FFO local oscillator signal can be measured up to 500 GHz that corresponds to the 27-th harmonic of the input signal from the synthesizer. The superfine resonance structure is present also in the measurements done by the external multiplier, and thus the resonances can be attributed to properties of the FFO rather than to the measuring method. Actually, Figs. 5-10 are recorded by using the external harmonic multiplier. Figure 9 shows the down-converted FFO signals with the FFO frequency locked - curve A- and phase locked – curve B). Note the extremely narrow linewidth ≈75 kHz was measured at a FFO frequency of 426 GHz - Fig. 9 (curve A) due to extremely low differential resistance. Actually, this is the linewidth of the free-running FFO since it was recorded with a very narrow (< 10 kHz) PLL regulation bandwidth that only suppresses low-frequency external interference without changing the FFO linewidth (frequency locking).

The external harmonic multiplier enables us to check an alternative concept of the Phase Locked Integrated Receiver. This concept [7] is based on an already proven design of the integrated receiver chip [1,2]. At this approach a submm-wave signal from an external harmonic multiplier driven by a 10 - 20 GHz synthesizer is applied to the integrated receiver via a beam splitter. A small portion of the IF band (about 50 MHz) is used to monitor the mixing product between the n-th harmonic of the synthesizer signal and the FFO signal. This down-converted signal after narrow-band filtering controls the PLL system while the rest of the IF band is used to analyze the down-converted signal.
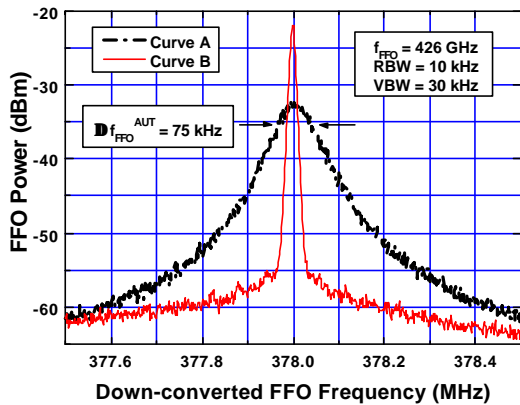
**Fig. 9.** Down-converted spectra of the FFO operated at 426 GHz; frequency locked (curve A) and phase locked (curve B).
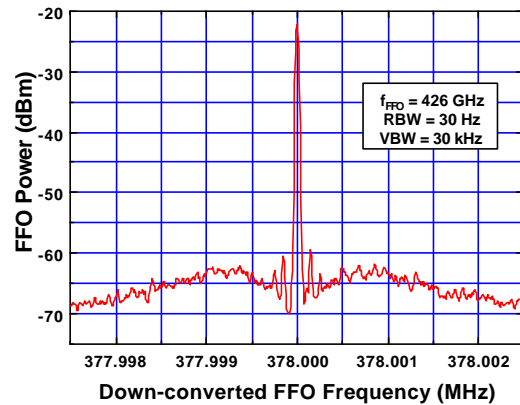
**Fig. 10.** Down-converted spectra of the phase locked FFO operated at 426 GHz, recorded at smaller IF span, see curve B in Fig. 9.

## 4. Discussion and conclusion

Preliminary tests demonstrate that there is no fundamental difference between results obtained by using either an integrated harmonic mixer or an external multiplier. The proper choice is a matter of convenience relevant for different applications. Phase locking of the FFO to an external reference oscillator is demonstrated experimentally using both measurement schemes. A FFO linewidth as low as 1 Hz (determined by the resolution bandwidth of the spectrum analyzer) has been obtained by both technique in the frequency range 270 - 440 GHz relative to a reference oscillator. To our knowledge it is the first time that the spectral linewidth of any Josephson device has been reduced so much by means of an electronic system. An observed superfine resonance structure in the FFO IVC reduces the FFO linewidth due to smaller differential resistance, but complicates FFO phase locking. In order to use the external multiplier with a thin beam splitter the multiplier output power at high harmonics must be increased at least 100 times. Here the development of a cryogenic multiplier looks very promising. The output power would be increased according to theoretical expectations, and a much thicker beam splitter can be used at cryogenic temperatures.

Implementation of the single-chip Superconducting Integrated Receiver with phase-lock-loop facilities is especially advantageous for new radio-astronomy projects based on an imaging array or multi-receiver approach (e. g., ALMA). The PLL Integrated Receiver is ready to be tested in the nearest future for practical spectral radio-astronomy in the frequency range 350 - 450 GHz. In this frequency range the Fiske steps of Nb-AlO$_x$-Nb FFOs are closely spaced and almost overlapping due to dissipation and dispersion in the long Josephson tunnel junction. The frequency gaps between the available LO bands (at subsequent FSs where FFO phase locking is possible), do not exceed 5 GHz. There is a possibility to gap these intervals using a receiver with a wide-band (4 GHz) IF amplifier while the FFO is biased and locked on an adjacent FS. This enables continuous in-phase-lock frequency coverage.

## References

1. S.V. Shitov, A.B. Ermakov, L.V. Filippenko, V.P. Koshelets, A.B. Baryshev, W. Luinge, Jian-Rong Gao, "Superconducting Chip Receiver for Imaging Applications", presented at ASC-98, Palm Desert, CA, USA, Report EMA-09, *IEEE Trans. on Appl. Supercond.,* **v.9,** No 2, pp. 3773-3776, (1999).

2. V.P. Koshelets, S.V. Shitov, "Integrated Superconducting Receivers", *Superconductor Science and Technology,* **vol 15**, No 5, pp. R1-R 17, (2000).

3. Nagatsuma, T., Enpuku, K., Irie, F., and Yoshida, K. 1983, Flux-Flow type Josephson oscillator for millimeter and submilimeter wave region, *J. Appl. Phys.* **54**, 3302-3309, see also Pt. II: 1984, *J. Appl. Phys.* **56**, p 3284; Pt. III: 1985, *J. Appl. Phys.* **58**, 441; Pt. IV: 1988, *J. Appl. Phys.* **63**, 1130.

4. Mygind, J., Koshelets, V.P., Shchukin, A.V., Shitov, S.V. and Lapytskaya, I.L. 1995, Properties of the autonomous and injection locked Flux-Flow Oscillators, *IEEE Trans. on Appl. Supercond*. **5**, 2951-2954.

5. Koshelets, V.P., Shitov, S.V., Baryshev, A.M., Lapitskaya, I.L., Filippenko, L.V., van de Stadt, H., Mess, J., Schaeffer, H. and de Graauw, T. 1995, Integrated sub-mm wave receivers, *IEEE Trans. on Appl. Supercond*. **5**, 3057-3060.

6. V.P. Koshelets, S.V. Shitov, A.V. Shchukin, L.V. Filippenko, and J. Mygind, "Linewidth of submillimeter wave flux flow oscillators", *Appl. Phys. Lett.,* vol. 69, pp. 699-701, July 1996.

7. V.P. Koshelets, A.M. Baryshev, J. Mygind, V.L. Vaks, S.V. Shitov, L.V. Filippenko, P.N. Dmitriev, W. Luinge, N. Whyborn, "Externally Phase Locked Sub-MM Flux Flow Oscillator for Integrated Receiver ", presented at EUCAS'99, report 8D-2, Barcelona, September (1999).

8. V.P. Koshelets, S.V. Shitov, L.V. Filippenko, V.L. Vaks, J. Mygind, A.B. Baryshev, W. Luinge, N. Whyborn, " Phase Locking of 270-440 GHz Josephson Flux Flow Oscillator", *Rev. of Sci. Instr.,* **v. 71,** No1, pp. 289-293, (2000).

9. V.P. Koshelets, S.V. Shitov, A.V. Shchukin, L.V. Filippenko, J. Mygind and A.V. Ustinov, "Self-pumping effects and radiation linewidth of FFO," *Phys. Rev. B,* vol. 56, pp. 5572- 5577, Sept. 1997.

10. M. Cirillo, N. Grønbech-Jensen, M. Samuelsen, M. Salerno, and G. Verona Rinati, "Fiske modes and Eck steps in long Josephson junctions: Theory and Experiments", Phys. Rev. B, vol. 58, pp. 12 377-12 384, 1998.

11. A.V. Ustinov, private communication.

12. E. Schomburg, R. Scheuerer, S. Brandl, K.F. Renk, D.G. Paveliev, Yu. Koschurinov, V. Ustinov, A. Zhukov, A. Kovsh, P.S. Kop`ev, *Electronics Letters,* Vol.35, No.17 (1999).